THE JOURNAL OF BIOLOGICAL CHEMISTRY Vol. 279, No. 36, Issue of September 3, pp. 37377–37384, 2004

Printed in U.S.A.

Molecular Cloning, Expression, and Properties of an Unusual Aldo-Keto Reductase Family Enzyme, Pyridoxal 4-Dehydrogenase, That Catalyzes Irreversible Oxidation of Pyridoxal*

Received for publication, May 13, 2004, and in revised form, June 11, 2004
Published, JBC Papers in Press, June 29, 2004, DOI 10.1074/jbc.M405344200

Nana Yokochi‡, Yu Yoshikane‡, Yanee Trongpanich‡, Kouhei Ohnishi‡§, and Toshiharu Yagi‡¶

From the ‡Department of Bioresources Science, Faculty of Agriculture and §Research Institute of Molecular Genetics, Kochi University, Monobe-Otsu 200, Nankoku, Kochi 783-8502, Japan

Microbacterium luteolum **YK-1 has pyridoxine degradation pathway I. We have cloned the structural gene for the second step enzyme, pyridoxal 4-dehydrogenase. The gene consists of 1,026-bp nucleotides and encodes 342 amino acids. The enzyme was overexpressed under cold shock conditions with a coexpression system and chaperonin GroEL/ES. The recombinant enzyme showed the same properties as the *M. luteolum* enzyme. The primary sequence of the enzyme was 54% identical with that of D-*threo*-aldose 1-dehydrogenase from *Agrobacterium tumefaciens*, a probable aldo-keto reductase (AKR). Upon multiple alignment with enzymes belonging to the 14 AKR families so far reported, pyridoxal 4-dehydrogenase was found to form a new AKR superfamily (AKR15) together with *A. tumefaciens* D-*threo*-aldose 1-dehydrogenase and *Pseudomonas* sp. L-fucose dehydrogenase. These enzymes belong to a distinct branch from the two main ones found in the phylogenic tree of AKR proteins. The enzymes on the new branch are characterized by their inability to reduce the corresponding lactones, which are produced from pyridoxal or sugars. Furthermore, pyridoxal 4-dehydrogenase prefers NAD^+ to $NADP^+$ as a cofactor, although AKRs generally show higher affinities for the latter.**

Pyridoxal 4-dehydrogenase (EC 1.1.1.107) catalyzes the oxidation of pyridoxal (pyridoxal hemiacetal) to 4-pyridoxolactone with NAD^+ (Fig. 1) and is the second enzyme in degradation pathway I for pyridoxine, one of the free forms of vitamin B_6, in which pyridoxine is degraded through eight enzyme-catalyzed steps to succinic semialdehyde, ammonia, and carbon dioxide (1). Pyridoxal 4-dehydrogenase has been purified partially and homogeneously from *Pseudomonas* MA-1 (2) and *Microbacterium luteolum* (3), respectively. The enzyme only catalyzes the dehydrogenase (oxidation) reaction on pyridoxal, and no reverse reduction of 4-pyridoxolactone has been observed (2, 3), although due to the low purity of the enzyme preparation (2) and the limited usage of the purified preparation (3), reexamination of the results is required. The reaction specificity suggests that the enzyme is a member of the aldehyde dehydrogenase family (4). However, the amino-terminal amino acid sequence of the enzyme protein showed no homology to the proteins in this family (3).

The aldo-keto reductases (AKRs)[1] comprise one of the three enzyme superfamilies that encompass NAD(P)(H)-dependent oxidoreductases (5), which can use aldehydes as substrates. They catalyze the reduction of aldehydes, ketones, monosaccharides, ketosteroids, and prostaglandins. Although AKRs also catalyze the oxidation of hydroxysteroids and *trans*-dehydrodiols of polycyclic aromatic hydrocarbons, they generally show much higher activity as to the reduction of aldehydes than the dehydrogenation (oxidation) of the corresponding alcohols (6). This superfamily contains more than 100 enzymes, which are divided into 14 families (AKR1–AKR14). They possess the (α/β) eight-barrel motif characteristic of triose-phosphate isomerases and contain ~320 amino acids/monomer. The majority of known AKRs are monomeric. However, multimeric forms are found in the AKR2, AKR6, and AKR7 families.

Here we have cloned the gene encoding pyridoxal 4-dehydrogenase from *M. luteolum* YK-1, developed an overexpression system for the recombinant pyridoxal 4-dehydrogenase in *Escherichia coli*, and examined the properties of the purified recombinant enzyme. *M. luteolum* pyridoxal 4-dehydrogenase exhibits 54% amino acid sequence identity with the probable AKR protein D-*threo*-aldose 1-dehydrogenase (EC 1.1.1.122) (7) and less than 40% similarity with other AKRs. Pyridoxal 4-dehydrogenase forms a new AKR family (AKR15) and belongs to a new branch, distinct from the two main branches, in the phylogenic tree of AKR proteins (5).

EXPERIMENTAL PROCEDURES

Bacterial Strains, Plasmids, and Cultivation—M. luteolum YK-1 (IFO 16738) isolated from soil was aerobically cultured at 30 °C in pyridoxine medium as described previously (3) and used as a DNA donor and for preparation of *M. luteolum* pyridoxal 4-dehydrogenase. *E. coli* JM109 (TaKaRa Bio) was used for cloning of the enzyme-coding gene or for expression of the recombinant enzyme, and *E. coli* BL21(DE3) (Novagen) was used for overexpression of the enzyme. *E. coli* cells were cultured in LB medium (1% polypeptone, 0.5% yeast extract, and 1% sodium chloride (w/v)) containing an adequate antibiotic or combination of antibiotics. Plasmids p3T (Mo Bi Tec), pET21a (Novagen), and pTrc99A (Amersham Biosciences) were used as the cloning and expression vectors, respectively. Plasmid pKY206 carrying *groEL/ES* genes (8) was obtained from Dr. M. Ashiuchi (Kochi University) and Dr. Y. Kawata (Tottori University). This plasmid was used as a coexpression vector.

Determination of Internal Amino Acid Sequence of Purified M. luteolum Pyridoxal 4-Dehydrogenase—The *M. luteolum* enzyme was purified as described previously (3). The purified enzyme or the recombi-

* The costs of publication of this article were defrayed in part by the payment of page charges. This article must therefore be hereby marked "*advertisement*" in accordance with 18 U.S.C. Section 1734 solely to indicate this fact.

The nucleotide sequence(s) reported in this paper has been submitted to the DDBJ/GenBank™/EBI Data Bank with accession number(s) AB092836.

¶ To whom correspondence should be addressed: Dept. of Bioresources Science, Faculty of Agriculture, Kochi University, Nankoku, Kochi 783-8502, Japan. Tel./Fax: 81-88-864-5191; E-mail: yagito@cc.kochi-u.ac.jp.

[1] The abbreviation used is: AKR, aldo-keto reductase.

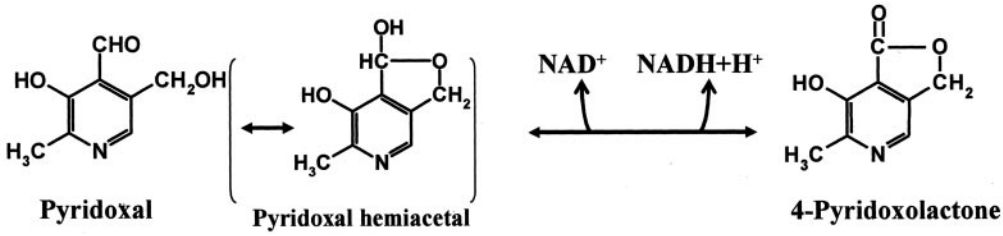

FIG. 1. **The enzyme reaction catalyzed by pyridoxal 4-dehydrogenase.**

nant enzyme prepared as described below (74 μg) was digested at 25 °C for 26 h with V-8 protease in a reaction mixture comprising 0.1 M Tris-HCl, pH 7.8, containing 2 M urea. The peptides were separated on an ODS-AM (YMC, 100 × 4.6 mm, 120 Å) reverse-phase column. Amino acid sequencing of the peptides was performed with an Applied Biosystems 492 protein sequencer.

Cloning of the Pyridoxal 4-Dehydrogenase Gene—Nearly half of the gene (*pld1*) encoding pyridoxal 4-dehydrogenase, which encodes the amino-terminal part of the enzyme protein, was amplified by PCR. Chromosomal DNA of *M. luteolum* YK-1 prepared by the method of Saito and Miura (9) was used as the template. The degenerate PCR primers designed based on the amino-terminal and internal sequences of the enzyme shown in Fig. 1 were 5′-GA(A/G)AA(A/G)CG(G/T/C)GC(A/G/T/C)CT(G/T/C)GG(A/G/T/C)CG(G/T/C)AC (A/G/C)-3′ and 5′-AA(A/G/T/C)CC(A/G/T/C)CC(A/G/T/C)CC(A/G/T/C)C(G/T)(A/G/T/C)GT-3′, respectively. The PCR conditions, with TaKaRa LA *Taq* polymerase and GC buffer I, were essentially the same as those described previously (10). The nucleotide sequence of the amplified DNA fragment (507 bp from the 5′-end of *pld1*) was determined with an Applied Biosystems 373 DNA sequencer.

The inverse PCR method was used for cloning the residual region of the *pld1* gene. The chromosome DNA of *M. luteolum* was digested with EcoRI, and then EcoRI-digested fragments were self-ligated to produce circular fragments. The latter were used as templates for PCR with primers 5′-AGGCACGAGTTTCACTGGAA-3′ (complementary to the antisense strand at nucleotide 484) and 5′-GCAGTTCCCAGAC-CAAGCGC-3′ (complementary to the sense strand at nucleotide 77).

The 3′-end of the *pld1* gene was cloned by cassette ligation-mediated PCR with a TaKaRa LA PCR *in vitro* cloning kit. PCR was performed essentially in the same way as described previously (10). The DNA fragment (about 3 kb) containing the 3′-end was amplified. Nucleotide sequencing of the DNA fragment clarified the entire sequence of the *pld1* gene.

The *pld1* gene was amplified by PCR with the chromosomal DNA from *M. luteolum* as a template. Primers 5′-CATATGCATTTGAAAG-CATCCGAG-3′ and 5′-GGATCCTGTCGAGGCGGAAAATGGTGT-3′ with a NdeI site (underlined in the former) and a BamHI site (underlined in the latter), respectively, were used. The amplified DNA fragment was ligated into p3T for TA cloning. The constructed plasmid, p3TPLD, was introduced into and extracted from *E. coli* JM109. After the sequence of the introduced fragment had been verified, p3TPLD was digested with NdeI and BamHI, and then the digested DNA fragment was inserted in the NdeI/BamHI sites of pET21a. The constructed plasmid, designated as pETPLD, was introduced into *E. coli* BL21(DE3). pETPLD was digested with XbaI and HindIII to obtain a DNA fragment containing the Shine-Dàlgàrno sequence in pET21a and the *pld1* gene. This fragment was inserted into the XbaI/HindIII sites of pTrc99A to construct pTRPLD, which was then introduced into *E. coli* JM109.

Expression of Pyridoxal 4-Dehydrogenase and Preparation of Crude Extracts—BL21(DE3)/pETPLD and JM109/pTRPLD cells were cotransformed with plasmid pKY206 carrying the GroEL/ES gene that encodes chaperonins, GroEL and ES, and increases the amount of the active form of the recombinant enzyme in the host cells (8). The cotransformants were grown in LB broth containing ampicillin (50 μg/ml) plus tetracycline (25 μg/ml) for 48 h at 23 °C. To examine the effect of induction with isopropyl-1-thio-β-D-galactopyranoside, 1 mM isopropyl-1-thio-β-D-galactopyranoside was added to the culture when the absorbance at 600 nm reached 0.6–0.8.

Cells were harvested and washed with 50 mM potassium phosphate buffer, pH 8.0, and then suspended in 20 mM potassium phosphate buffer, pH 8.0, containing 0.1% (v/v) 2-mercaptoethanol, 10% (w/v) glycerol, 1 mM EDTA, and 1 mM phenylmethylsulfonyl fluoride (Buffer A containing phenylmethylsulfonyl fluoride). The cell suspension was thoroughly sonicated at 4–15 °C with a Heat Systems-Ultrasonics sonicator W-220. The precipitate containing cell debris and insoluble materials was removed by centrifugation at 10,000 × *g* for 10 min at 4 °C, and the supernatant was used as the soluble fraction. The precipitate was mixed with Buffer A containing 6 M urea, and then the mixture was kept on ice for 2 h and centrifuged to remove insoluble materials. The supernatant containing the dissolved inclusion proteins was used as the dissolved fraction.

Purification of Recombinant Pyridoxal 4-Dehydrogenase—The cotransformant cells (4.7 g), BL21(DE3)/pETPLD/pKY206, were suspended in 25 ml of Buffer A containing 1 mM phenylmethylsulfonyl fluoride. The suspension was sonicated on ice for 15 min with a Heat Systems-Ultrasonicator W-220. The supernatant (40 ml) obtained on centrifugation at 10,000 × *g* for 20 min at 4 °C was used as the crude extract. The crude extract was fractionated with ammonium sulfate, and the precipitate obtained upon centrifugation of the 40–70% saturated solution was dissolved in 14 ml of Buffer A. This solution, after dialysis against Buffer A, was applied to a Blue A (Amicon) column (1.8 × 8.0 cm) equilibrated with Buffer A. The column was washed with Buffer A and then Buffer A containing 0.1 M NaCl until the absorbance of the eluate at 280 nm become lower than 0.1. Then the enzyme was eluted with Buffer A containing 0.2 mM NAD^+ as a single peak.

Enzyme and Protein Assays—Pyridoxal 4-dehydrogenase was assayed during its purification by measuring the increase in fluorescence (excitation at 356 nm and emission at 432 nm) of 4-pyridoxolactone produced as described previously (3), for which 2–100 milliunits of the enzyme was routinely used. One unit of enzyme was defined as the amount that catalyzed the formation of 1 nmol of 4-pyridoxolactone per min (3). The reverse reaction was assayed by the phenylhydrazine method, in which pyridoxal produced was measured as phenylhydrazone (11), because a high concentration of 4-pyridoxolactone, which shows maximum absorbance at 356 nm, interfered with measurement of the decrease in the absorption of NADH. The reaction was performed in a reaction mixture (0.4 ml) consisting of 50 mM sodium phosphate buffer (pH 8.0), 50 mM 4-pyridoxolactone, 10 mM NADH, and 5 units of enzyme at 30 °C for 1 h. The reaction was stopped by the addition of 66 μl of 9 M sulfuric acid. The reaction mixture (0.3 ml) after centrifugation was mixed with 0.6 ml of 1 M sulfuric acid and 0.1 ml of 2% (w/v) phenylhydrazine (dissolved in 5 M sulfuric acid), and then the mixture was incubated at 60 °C for 20 min. The A_{410} of the mixture was measured. Protein was measured by the dye-binding method with bovine serum albumin as a standard (12).

Substrate Specificity of the Recombinant Enzyme—The enzyme activity toward sugars and the K_m values were determined by measuring the initial increase in A_{340} of NADH at 30 °C in 1.0 ml of a reaction mixture consisting of 50 mM sodium phosphate buffer (pH 8.0), 250 mM each sugar, 1.0 mM NAD^+, and the enzyme. The reactivity with aldehydes, which are typical synthetic AKR substrates, was measured in the same reaction mixture containing 1.0 mM each aldehyde instead of the sugar. The K_m value for pyridoxal was measured under the same conditions with the exception that A_{366} was followed instead of A_{340}. Kinetic parameters were determined as described previously (10).

Other Analytical Methods—The molecular weight of the recombinant enzyme was determined by gel filtration (Hiprep 16/60 Sephacryl S-300 high resolution column) with a fast protein liquid chromatograph. A calibration curve was made based on the elution pattern of catalase (M_r 240,000), lactate dehydrogenase (M_r 140,000), alanine aminotransferase (M_r 110, 000), malate dehydrogenase (M_r 72,000), and cytochrome *c* (M_r 12,400). The subunit molecular weight was measured by SDS-PAGE (13) with the molecular weight markers as described previously (10).

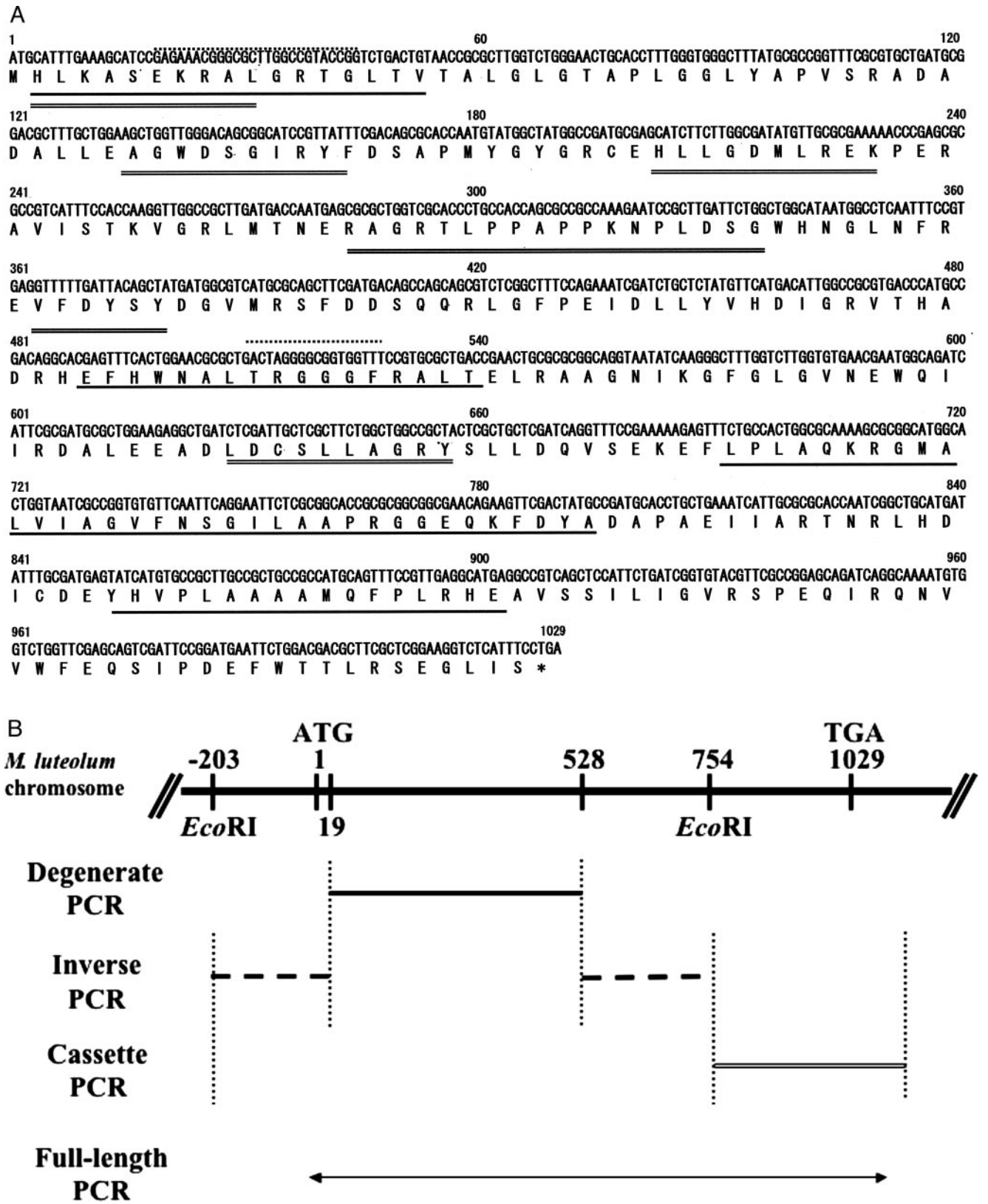

FIG. 2. **Cloning of the pyridoxal 4-dehydrogenase gene of *M. luteolum*.** *A*, the deduced amino acid sequence. The *solid underlines* and *double lines* show the N-terminal and internal amino acid sequences determined for the native enzyme and recombinant enzyme, respectively. The *dotted overlines* show amino acid residues used for the design of degenerate primers. *B*, the scheme of *pld1* gene cloning. The gene fragments were obtained by degenerate PCR (*solid line*), inverse PCR (*broken lines*), cassette-mediated PCR (*double line*), and full-length PCR (*line with arrowheads*).

RESULTS

Cloning of the M. luteolum Pyridoxal 4-Dehydrogenase Gene—The amino acid sequences of the amino-terminal region and three internal peptides generated on V-8 protease digestion were determined (*solid underlines* in Fig. 2*a*). Based on the amino acid sequence information, degenerate primers were

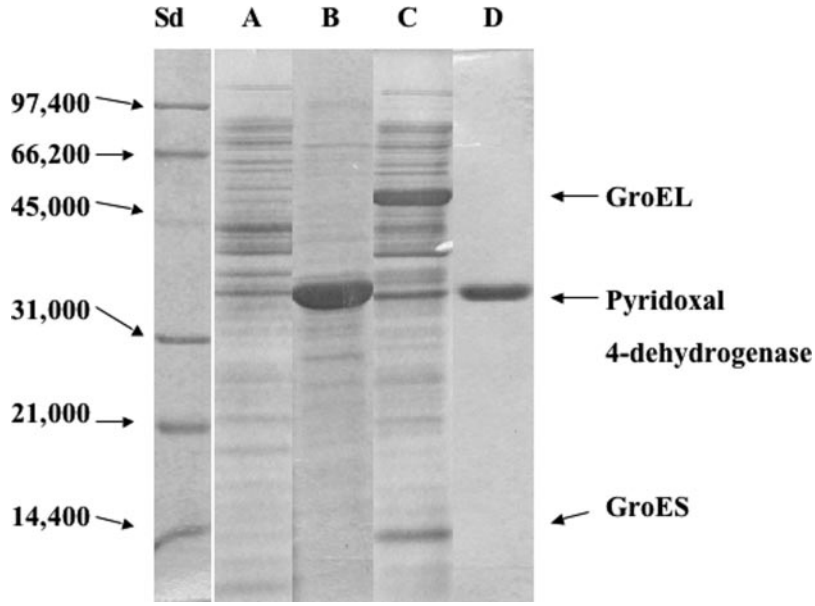

FIG. 3. **SDS-PAGE patterns of crude extracts of recombinant *E. coli* cells and the purified enzyme from BL21 (DE3)/pETPLD/pKY206 cells.** *Lane A*, crude extract (10 μg of protein) of BL21(DE3)/pETPLD cells; *lane B*, the dissolved inclusion proteins (10 μg) of BL21(DE3)/pETPLD cells; *lane C*, crude extract (10 μg) of BL21(DE)/pETPLD/pKY206 cells; *lane D*, the purified recombinant enzyme (2.2 μg). The standard proteins were applied to *lane Sd*.

TABLE I
Purification of pyridoxal 4-dehydrogenase from cotransformant E. coli cells

Fraction	Total protein	Total activity	Specific activity	Yield
	mg	*units*	*units/mg*	%
Crude extract	414	2,700	6.5	100
Ammonium sulfate	251	2,680	11.6	99.4
Blue A	2.6	1,670	635	62.3

TABLE II
Comparative reactivity of pyridoxal 4-dehydrogenase with sugars and pyridoxal

D-Xylose, L-arabinose, and D-galactose were not dehydrogenated by the enzyme. The K_m and K_{cat} values for pyridoxal were reexamined by means of the photometric assay in this study.

Compound	K_m	K_{cat}	K_{cat}/K_m
	mM	s^{-1}	$s^{-1}\ mM^{-1}$
Pyridoxal	13 ± 2.5	59.2 ± 7.3	4.6
L-Fucose	0.41 ± 0.05	125 ± 2.0	304.9
D-Arabinose	0.91 ± 0.08	175 ± 1.9	192.3
L-Xylose	3.5 ± 0.19	214 ± 1.4	6.1
NAD^+	0.042 ± 0.003		
$NADP^+$	0.58 ± 0.14		

designed for PCR, which corresponded to the amino acids indicated by *dotted lines* in Fig. 2*A*. The *pld1* gene fragment comprising nucleotides 19–528 was amplified by PCR (*thick line* in Fig. 2*B*). Upon inverse PCR with the circularized EcoRI-digested fragments, a 550-bp fragment was amplified, which contained the 5′-end and the central part of the *pld1* gene (*solid line* in Fig. 2*B*). Finally, the 3′-terminal region of the *pld1* gene was amplified by cassette ligation-mediated PCR, as shown by the *double line* in Fig. 2*B*. The entire *pld1* gene was amplified (Fig. 2*B*), and the nucleotide sequence was verified (Fig. 2*A*). The *pld1* gene consisted of 1,026 bp nucleotides, which encoded 342 amino acid residues (Fig. 2*A*). The predicted molecular mass was 37,889, which was in good agreement with the molecular mass (38,000) determined previously by SDS-PAGE (3).

Expression of the pld1 Gene in E. coli—The expression of the *pld1* gene in various *E. coli* transformants was examined with cells cultured in a small volume of medium (5.0 ml) under different conditions. BL21(DE3)/pETPLD and JM109/pTRPLD cells grown at 37 °C showed low pyridoxal 4-dehydrogenase activity (0.25 ± 0.05 and 0.26 ± 0.02 units/mg, respectively), which was almost the same value as that for *M. luteolum* grown in the pyridoxine synthetic medium. The amount of the enzyme protein was so low that the protein band could not be seen in the SDS-polyacrylamide gel (Fig. 3, *lane A*). Because the patterns of the protein bands on the gel were very similar for the two types of transformant cells, only the results for BL21(DE3)/pETPLD cells are shown in Fig. 3. Both types of cells showed the formation of large amounts of insoluble enzyme proteins (Fig. 3, *lane B*). To increase the soluble and active forms of the enzyme protein, BL21(DE3)/pETPLD cells were cultured under different conditions, such as cultivation at high (44 and 42 °C) or low (20 °C) temperature and induction with isopropyl-1-thio-β-D-galactopyranoside. Only cultivation at the low temperature was effective, the specific activity being increased to 1.28 ± 0.31 units/mg. Because it has been reported that the coexpression of *E. coli* chaperonin proteins increases the soluble forms of several enzymes (8, 14), we examined the effect of their coexpression on pyridoxal 4-dehydrogenase in the transformant cells. The specific activity of the enzyme in BL21(DE3)/pETPLD/pKY206 cells and JM109/pTRPLD/pKY206 cells, which were cultured without isopropyl-1-thio-β-D-galactopyranoside at 23 °C, was 11.8 ± 3.24 and 14.6 ± 1.55 (*i.e.* 9.2- and 8.8-fold higher than the values for BL21(DE3)/pETPLD cells and JM109/pTRPLD cells, respectively). The amount of the soluble form of the enzyme was high enough to see it in the SDS-polyacrylamide gel as a protein band (Fig. 3, *lane C*). Thus, cold stress and cooperative expression of chaperonins increased the soluble and active forms of pyridoxal 4-dehydrogenase in the host cells. Both types of cells could be used for purification of the enzyme.

Purification and Properties of Recombinant Pyridoxal 4-Dehydrogenase—The recombinant pyridoxal 4-dehydrogenase was purified to homogeneity from BL21(DE3)/pETPLD/pKY206 cells by one-step column chromatography (Fig. 3, *lane D*, and Table I). The specific activity of the crude extract used as the starting material was lower than that observed in the transformant cells cultivated in a small volume (5 ml). For an unknown reason, the transformant cells showed lower specific activity when they were grown in a larger volume (200 ml) for preparation of the enzyme.

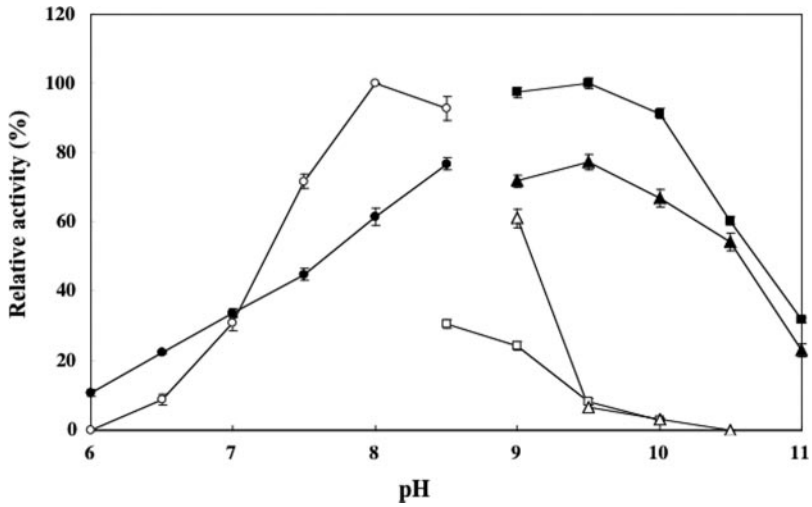

FIG. 4. **Differences in optimum pH of pyridoxal 4-dehydrogenase.** When pyridoxal was used as the substrate, measurements were made in 50 mM sodium phosphate buffer (*open circles*), CAPS-KOH (*open triangles*), or sodium bicarbonate-bicarbonate (*open squares*) containing 1 mM NAD^+ and 0.5 mM pyridoxal. The reaction with L-fucose was examined in 50 mM sodium phosphate buffer (*closed circles*), CAPS-KOH (*closed triangles*), or sodium bicarbonate-carbonate (*closed squares*) containing 1 mM NAD^+ and 4 mM L-fucose. The averages and S.D. of three experiments are shown.

```
                1                                                  50                                                 100
PL dehydrogenase MHLKASEKRALGRTGLTVTALGLGTAPLGGLYAPVSRADADALLEAGWDSGIRYFDSAPMYGYGRCEHLLGDMLREKP---ERAVISTKVGRLMTNERAGRTL
Agrobacterium    --MRAGDKRRLGTTNLSVTALSMGCASLGGLYTPVSAADALATLQAAWDSGVRYFDVAPMYGLTRAEHLLGQFLREEPQC-HEAVVSTKVGRLFSNDRPGHRL
Pseudomonas      ---MSSTEPAAAAAGLAIPALGYGAANVGNLFRALSDDEAWAVLEAAWDAGIRYYDTAPHYGLGLSEKRLGAFLQTKPR--DEFVVSTKAGRLLR--------
Candida          --MSASIPDIKLSSGHLMPSIGFGCWKLAN-------ATAGEQVYQAIKAGYRLFDGAEDYGN---EKEVGDGVKRAID---EGLVKREEIFLTSKLWNNYHD
Rat              ----------MSQARPATVLGAMEMGRRMDVTS---SSASVRAFLQRGHTEIDTAFVYANGQSETILGDLGLGLGRSGCKVKIATKAAPMFG-----KTL

                                                  150
PL dehydrogenase PPAPPKNP--LDSG--WHNGLNFREVFDYSYDGVMRSFDDSQQRLGFPEIDLLYVHDIGRVTHADRHEFHWNALTRGGG----------FRALTELRAAG
Agrobacterium    PPEPPKNP--LDPG--WQNGLPFRETFDYSYDGIMRSFDDSQQRMGTNRLDILFIHDIGVLTHGERNAALWRQLTSGG----------FRALGELREAG
Pseudomonas      -PNPERRPSGLDTDNDFHVPDDLRREWDFTEQGIRASIAESQERLGLDRIDLLYLHDP---------ERHDLDLALASA----------FPALEKVRAEG
Candida          PKNVETALN----------KTLAD----------LKVDYVDLFLIHFPIAFKFVPIEEKYPPGFYCGDGNNFVYEDVPILETWKALEKLVAAG
Rat              KPADVRFQLET----------SLKRLQCPRVDLFYLHFPDHGTP----------IEETLQACHQLHQEG

                        200                                                250
PL dehydrogenase NIKGFGLG-----VNEWQIIRDALEEADLDCSLLAGRYS-LLDQVSEKEFLPLAQKRGMALVIAG-----VFNSGILAAPRGGEQKFD----------
Agrobacterium    LIGGFGLG-----VNEAEAIAAAMDEVHLDCCLLAGRHS-LLEQDAVP-LLDRAHRQGTAIVIGG-----VFNSGILATGTASNAKFN----------
Pseudomonas      VVKAIGIG-----SMVSDALTRAVREADLDLIMVAGRYT-LLEQPAATEVLPACAENATGIVAAS-----VFNSGLLAQ---SEPKRDGR----------
Candida          KIKSIGVS-----NFPGALLLDLLRGATIKPAVLQVEHHPYLQQPKLIEFAQKAGVTITAYSSFGPQSFVEMNQGRALNTPTLFAHDTIKAIA----------
Rat              KFVELGLSNYVSWEVAEICTLCKKNGWIMPTVYQGMYN-AITRQVETELFPCLRHFGLRFYAFN-----PLAGGLLTGRYKYQDKDGKNPESRFFGNPFSQLY

                                  300
PL dehydrogenase ---YADAPAEIIARTNRLHDICDEYHVP---LAAAAMQ-----FPLRHEAVSSILIGVRSPEQIRQNVVWFEQS---IPDEFWTTLRSEGLIS--------
Agrobacterium    ---YKDAPAEIVRRTEELARVCAAFDVP---LGAAAVQ-----FPLFHPAVASVLVGAKHPDKLLQSVGWFETD---IPEELWQALQKKGLLAPMPVLMET
Pseudomonas      -YEYGQLPDELWDRLVRIAAICRNHDVP---LPAAAIQ-----FPLQSALVRSVVVGGSRPAQLTQNAEYAALE---IPAGLWAELAEARLIPTP------
Candida          -AKYNKTPAEVLLRWAAQRGIAVIPKSN---LPERLVQNRS---FNTFDLTKEDFEEIAKLDIGLRFNDPWDWDN---IPIFV----------
Rat              MDRYWKEEHFNGIALVEKALKTTYGPTAPSMISAAVRWMYHHSQLKGTQGDAVILGMSSLEQLEQNLALVEEGPLEPAVVDAFDQAWNLVAHECPNYFR
```

FIG. 5. **Alignment of the amino acid sequences of pyridoxal 4-dehydrogenase and some other AKRs.** The sequence (PL dehydrogenase; AKR15A) was aligned by means of the ClustalW multiple sequence alignment program with those of the putative D-*threo*-aldose 1-dehydrogenase of *A. tumefaciens* (*Agrobacterium*), L-fucose dehydrogenase of *Pseudomonas* sp. (*Pseudomonas*), xylose reductase of *C. tenuis* (*Candida*; AKR2B5), and aflatoxin dialdehyde reductase of rat (*Rat*; AKR7A1). An amino acid residue common to four or five sequences is shown in *boldface type*. The amino acid residues involved in the binding of $NADP^+$ and the formation of the active sites and dimeric structure are shown by *highlighted*, *outlined*, and *underlined letters*, respectively, in the sequences of xylose reductase and aflatoxin dialdehyde reductase.

The purified recombinant enzyme showed 1.8-fold higher specific activity than the *M. luteolum* enzyme. However, the optimum pH (pH 8.0), the optimum temperature (30 °C), the thermostability (75% inactivation at 45 °C for 10 min), and the molecular weights both on gel filtration (84,000 ± 4,200) and SDS-PAGE (38,000 ± 600) were the same for the recombinant and native enzymes. Pyridoxal 4-dehydrogenase is a dimeric protein. The amino-terminal 10-amino acid sequence and the sequences of five V8-cleaved peptides derived from the recombinant enzyme were determined (the *double lines* in Fig. 2*A*). Whereas the amino-terminal methionine was removed in the recombinant enzyme, the determined amino acid sequences coincided with those deduced from the nucleotide sequences.

Activity toward Sugars and Aldehydes—Because the primary sequence of pyridoxal 4-dehydrogenase was similar to

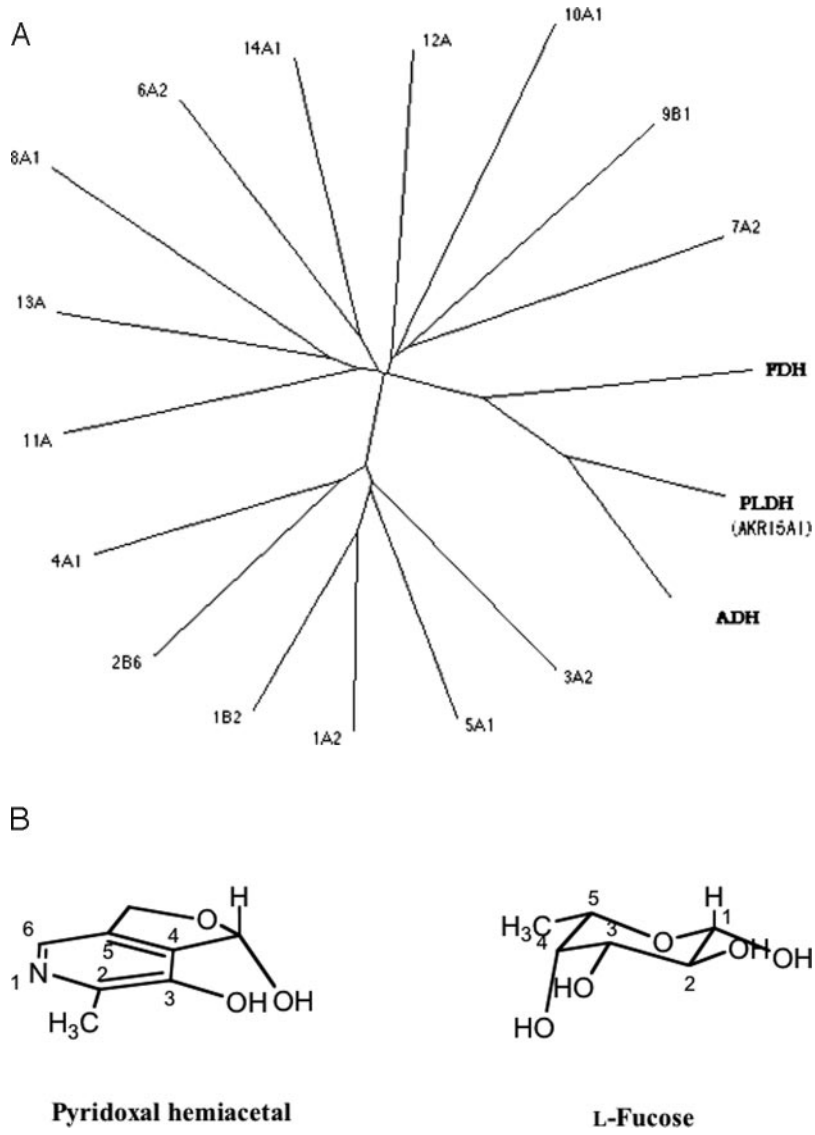

FIG. 6. **Unrooted phylogenic tree of aldo-keto reductases and the conformations of pyridoxal hemiacetal and the β-anomer of L-fucose.** *A*, a representative AKR was selected from each family. AKR1A2, -1B2, -2B6, -3A2, -4A1, -5A1, -6A2, -7A2, -8A1, -9B1, -10A1, -11A, -12A, -13A, and -14A1 are aldehyde reductase, aldose reductase, Gre 3p, Ypr1p, chalcone polyketide reductase, reductase, shaker channel β-subunit, aflatoxin inducible aldehyde reductase, pyridoxal reductase, aryl-alcohol dehydrogenase, bluensomycin aldo-keto reductase, vegetative protein, NDP-hexose-2, 3-enoyl reductase, YakC aldo-keto reductase, and *E. coli* aldehyde reductase, respectively. PLDH, ADH, and FDH are *M. luteolum* pyridoxal 4-dehydrogenase, *A. tumefaciens* D-*threo*-aldose 1-dehydrogenase, and *Pseudomonas* sp. L-fucose dehydrogenase, respectively. *B*, the conformations of pyridoxal hemiacetal (*left*) and the β-anomer of L-fucose (*right*) are shown.

that of a putative D-*threo*-aldose 1-dehydrogenase, the reactivity of the enzyme with sugars was examined. The enzyme showed high activity toward L-fucose, D-arabinose, and L-xylose (Table II). These substrates have hydroxyl groups at the second and third carbons in the *threo* configuration. The substrates showed Michaelis-Menten type kinetics. L-Fucose was the best substrate, having the highest specificity constant.

When L-fucose was used as the hydrogen donor, the optimum pH of the enzyme reaction was pH 9.5 (Fig. 4). In contrast, it was pH 8.0 when pyridoxal was used. Whereas carbonate buffers inhibited the dehydrogenation of pyridoxal, they did not inhibit that of L-fucose. The optimum temperature was 45 °C, and the enzyme was stable up to 40 °C when L-fucose was used as the substrate. Whereas no difference was observed in thermostability between the enzyme reactions with L-fucose and pyridoxal, the optimum temperature was 10 °C higher with L-fucose than with pyridoxal. The K_m values for NAD^+ were 0.042 ± 0.003 and 0.05 ± 0.004 mM with L-fucose and pyridoxal as the substrate, respectively. The K_m value for $NADP^+$ determined with L-fucose was 0.58 ± 0.14 mM.

Pyridoxal 4-dehydrogenase showed no measurable activity toward benzaldehyde, 2-nitrobenzaldehyde or 4-nitrobenzaldehyde although these synthetic aldehydes are good substrates for AKRs so far studied (15).

DISCUSSION

M. luteolum pyridoxal 4-dehydrogenase shows the highest identity (54%) with a probable D-*threo*-aldose 1-dehydrogenase in *Agrobacterium tumefaciens* (AAL44626, 348 residues). *Mesorhizobium loti* putative D-*threo*-aldose 1-dehydrogenase (BAB50246, 332 residues), *Sinorhizobium meliloti* putative protein (AAK65425, 338 residues), *S. meliloti* putative L-fucose dehydrogenase (CAC41406, 339 residues), *M. loti* unknown protein (BAB54355, 340 residues), *Bradyrhizobium japonicum* putative oxidoreductase (BAC46389, 325 residues), *Pseudomonas* sp. L-fucose dehydrogenase (BAA06803, 329 residues), and *Bacillus anthracis* str. Ames oxidoreductase (AAP27231, 336 residues) show identities of 45, 44, 42, 40, 39, 38, and 37%, respectively. Since D-*threo*-aldose 1-dehydrogenase is a potential member of the AKR superfamily (16), *M. luteolum* pyridoxal 4-dehydrogenase could belong to the AKR superfamily.

The amino acid sequence of pyridoxal 4-dehydrogenase was aligned with those of *A. tumefaciens* D-*threo*-aldose 1-dehydrogenase, *Pseudomonas* sp. L-fucose dehydrogenase (17), *Candida tenuis* xylose reductase (AKR2B7) (18), and rat aflatoxin dialdehyde reductase (AKR7A1) (19) (Fig. 5). *C. tenuis* xylose reductase and rat aflatoxin dialdehyde reductase are novel dimeric members of the AKR superfamily with defined tertiary

structures. All of the residues in the active sites of AKRs are conserved in pyridoxal 4-dehydrogenase, namely Asp-56, Tyr-61, Lys-86, and His-152, corresponding to Asp-40, Tyr-45, Lys-73, and His-109 in the AKR7A1 protein, respectively (Fig. 5). The amino acid residues involved in $NAD(P)^+$ binding are also conserved, namely Gly-250, Arg-256, Gln-315, Gln-318, and Asn-319, corresponding to Gly-198, Arg-204, Glu-290, Glu-293, and Asn-294 in the AKR7A1 protein, respectively (Fig. 5). Therefore, *M. luteolum* pyridoxal 4-dehydrogenase is a member of the AKR superfamily.

The AKR superfamily, so far, comprises 14 families. A representative was selected from each family and aligned with *M. luteolum* pyridoxal 4-dehydrogenase, *A. tumefaciens* D-*threo*-aldose 1-dehydrogenase, and *Pseudomonas* sp. L-fucose dehydrogenase. Enzymes belonging to one family exhibit less than 40% amino acid sequence identity with enzymes belonging to other families (16). No enzymes in the 14 families show more than 40% amino acid sequence identity with pyridoxal 4-dehydrogenase. When an unrooted phylogenic tree was constructed, pyridoxal 4-dehydrogenase was found to form a distinct branch together with two aldose reductases (Fig. 6*A*). These two aldose reductases show reactivity with aldoses with hydroxyl groups at the 2- and 3-positions with the *threo* configuration. From these data, we propose a new AKR family, which is composed of pyridoxal 4-dehydrogenase and other aldose reductases. The sequence of pyridoxal 4-dehydrogenase was submitted to the AKR superfamily homepage (available on the World Wide Web at www.med.upenn.edu/akr/), and the new family was designated as AKR family 15.

The phylogenic tree of the AKR superfamily has two major branches; one branch is composed of AKR families 1–5, and the other is composed of AKR families 6–14 (5) (Fig. 6*A*). The pyridoxal 4-dehydrogenase family, family 15, forms a third major branch. Enzymes in family 15 are different from the others in several biochemical properties as well. They only catalyze the oxidation (dehydrogenation) reaction and have a dimeric structure, and some of them show higher affinity for NAD^+ than for $NADP^+$. Pyridoxal 4-dehydrogenase showed no reactivity with 4-pyridoxolactone even when the lactone concentration was 50 mM and a 100-fold higher amount of the enzyme was used. The effective irreversibility of the enzyme reaction has also been found for *Pseudomonas* pyridoxal 4-dehydrogenase (2). L-Fucose dehydrogenase from rabbit liver belonging to the AKR family 15 shows no catalytic activity toward L-fuconolactone (20). This irreversibility is attributed to spontaneous hydrolysis of L-fuconolactone at basic pH because the enzyme shows an optimum pH of 10.0. However, this is not the case for pyridoxal 4-dehydrogenase, because the enzyme shows an optimum pH of 8.0–8.5, where 4-pyridoxolactone is not easily hydrolyzed. The inability of family 15 enzymes to reduce lactones may cause controversy regarding the molecular evolution of AKRs. Further studies are required to elucidate the mechanism involved.

AKRs generally show only affinity for $NADP^+$ or higher affinity for $NADP^+$ than for NAD^+ when both coenzymes are used as cofactors, although a NAD-preferring xylose reductase has recently been characterized (21). Codeinone reductase (AKR4B2), morphine dehydrogenase (AKR5B), pyridoxal reductase (AKR8A1), and aryl-alcohol dehydrogenase (AKR9A3) can only use $NADP^+$. Ara1p-arabinose dehydrogenase (AKR3C), shaker channel β-subunit (AKR6A1), and aldehyde reductase (AKR1A2) show 3–10-fold higher affinity for $NADP^+$ than for NAD^+, respectively. On the contrary, pyridoxal 4-dehydrogenase showed 10-fold higher affinity for NAD^+ than for $NADP^+$ as the xylose reductase (21).

Although the majority of AKRs are monomeric, recent studies have shown that xylose reductase (AKR2B5) (6) and aflatoxin-inducible aldehyde reductase (AKR7A1) (22) are dimeric. *M. luteolum* pyridoxal 4-dehydrogenase in AKR15 was shown to be dimeric. The amino acid residues necessary for dimerization of *C. tenuis* xylose reductase, Asp-178, Glu-205, Phe-206, Trp-313, and Pro-319, are well conserved as Asp-203, Glu-229, Phe-230, Trp-322, and Pro-328 of pyridoxal 4-dehydrogenase (Fig. 5). These residues in pyridoxal 4-dehydrogenase are likely to be involved in dimer formation.

L-Fucose was a better substrate for pyridoxal 4-dehydrogenase than pyridoxal. Although several L-fucose dehydrogenases (EC 1.1.1.122, D-*threo*-aldose 1-dehydrogenase) from animals and microorganisms have been characterized, their reactivity with pyridoxal has not been reported. L-Fucose dehydrogenase from porcine liver acts on the β-anomer of L-fucose and catalyzes hydride transfer of the C-1 hydrogen axial in the lowest energy chair conformation (23). Korytnyk and Singh (24) have found that pyridoxal existed exclusively in the hemiacetal form at pD 1.0–11.0 by examining its proton magnetic resonance spectra. Interestingly, the conformations of pyridoxal hemiacetal and the chair form of L-fucose show several similarities between functional groups (Fig. 6*B*). When the conformational structures are placed one upon another at C-1 of L-fucose and C-4′ of pyridoxal hemiacetal, both of which bind the axial hydrogen to be released, the C-2 oxygen and C-3 oxygen in L-fucose and pyridoxal hemiacetal, respectively, occupy similar positions to the carbons. Furthermore, the C-3 oxygen of L-fucose is located at a similar position to the nitrogen of the pyridine ring in pyridoxal hemiacetal. Thus, it is possible that L-fucose and pyridoxal hemiacetal bind to the active site pocket of the enzyme, where some amino acid residues provide binding sites for these atoms through hydrogen bonds, and that the enzyme shows reactivity with the compounds. Indeed, the optimum pH of pyridoxal was lower than that of L-fucose, suggesting that the C-3 phenolic hydroxyl group in pyridoxal hemiacetal should be in a nondissociated form for binding to the binding site. The substrate-binding pocket of pyridoxal 4-dehydrogenase from *M. luteolum* may be similar to those of D-*threo*-aldose 1-dehydrogenases. Comparative studies on D-*threo*-aldose 1-dehydrogenase from different sources will provide the clues for understanding the molecular mechanism underlying the changes in the substrate specificities of AKR proteins.

REFERENCES

1. Nelson, M. J., and Snell, E. E. (1986) *J. Biol. Chem.* **261,** 15115–15120
2. Burg, R. W., and Snell, E. E. (1969) *J. Biol. Chem.* **244,** 2585–2589
3. Trongpanich, Y., Abe, K., Kaneda, Y., Morita, T., and Yagi, T. (2002) *Biosci. Biotechnol. Biochem.* **66,** 543–548
4. Achterholt, S., Priefert, H., and Steibuchel, A. (1998) *J. Bacteriol.* **180,** 4387–4391
5. Hyndman, D., Bauman, D. R., Heredia, V. V., and Penning, T. M. (2003) *Chem. Biol. Interact.* **143,** 621–631
6. Kavanagh, K. L., Klimacek, M., Nidetzky, B., and Wilson, D. K. (2002) *Biochemistry* **41,** 8785–8795
7. Wood, D. W., Setubal, J. C., Kaul, R., Monks, D. E., Kitajima, J. P., Okura, V. K., Zhou, Y., Chen, L., Wood, G. E., Almeida, N. F., Jr., Woo, L., Chen, Y., Paulsen, I. T., Eisen, J. A., Karp, P. D., Bovee, D., Sr., Chapman, P., Clendenning, J., Deatherage, G., Gillet, W., Grant, C., Kutyavin, T., Levy, R., Li, M. J., McClelland, E., Palmieri, A., Raymond, C., Rouse, G., Saenphimmachak, C., Wu, Z., Romero, P., Gordon, D., Zhang, S., Yoo, H., Tao, Y., Biddle, P., Jung, M., Krespan, W., Perry, M., Gordon-Kamm, B., Liao, L., Kim, S., Hendrick, C., Zhao, Z. Y., Dolan, M., Chumley, F., Tingey, S. V., Tomb, J. F., Gordon, M. P., Olson, M. V., and Nester, E. W. (2001) *Science* **294,** 2317–2323
8. Mizobata, T., Akiyama, Y., Ito, K., Yumoto, N., and Kawata, Y. (1992) *J. Biol. Chem.* **267,** 17773–17779
9. Saito, H., and Miura, K. (1963) *Biochim. Biophys. Acta* **72,** 619–629
10. Nakano, M., Morita, T., Yamamoto, T., Sano, H., Ashiuchi, M., Masui, R., Kuramitsu, S., and Yagi, T. (1999) *J. Biol. Chem.* **274,** 23185–23190
11. Kaneda, Y., Ohnishi, K., and Yagi, T. (2002) *Biosci. Biotechnol. Biochem.* **66,** 1022–1031
12. Bradford, M. M. (1976) *Anal. Chem.* **72,** 248–254
13. Laemmli, U. K. (1970) *Nature* **227,** 680–685

14. Yoshikane, Y., Yokochi, N., Ohnishi, K., and Yagi, T. (2004) *Protein Expression Purif.* **34,** 243–248
15. Morita, T., Huruta, T., Ashiuchi, M., and Yagi, T. (2002) *J. Biochem.* (*Tokyo*) **132,** 635–641
16. Joseph, M. J., and Trevor, M. P. (2001) *Chem. Biol. Interact.* **130,** 499–525
17. Yamamoto-Otake, H., Nakano, E., and Koyama, Y. (1994) *Biosci. Biotechnol. Biochem.* **58,** 2281–2282
18. Hacker, B., Habenicht, A., Kiess, M., and Mattes, R. (1999) *Biol. Chem.* **380,** 1395–1403
19. Ellis, E. M., Judah, D. J., Neal, G. E., and Hayes, J. D. (1993) *Proc. Natl. Acad. Sci. U. S. A.* **90,** 10350–10354
20. Endo, M., and Hiyama, N. (1979) *J. Biochem.* (*Tokyo*) **86,** 1559–1565
21. Lee, J.-K., Koo, B.-S., and Kim, S.-Y. (2003) *Appl. Environ. Microbiol.* **69,** 6179–6188
22. Kozma, E., Brown, E., Ellis, E. M., and Lapthorn, A. J. (2002) *J. Biol. Chem.* **277,** 16285–16293
23. Berkowitz, D. B., and Benner, S. A. (1987) *Biochemistry* **26,** 2606–2611
24. Korytnyk, W., and Singh, R. P. (1963) *J. Am. Chem. Soc.* **85,** 2813–2817